ISSN : 0974 - 7524 Volume 9 Issue 7

Physical CHEMISTRY
An Indian Journal

Full Paper

PCAIJ, 9(7), 2014 [225-238]

Oxide film formation and growth on indium electrode in $Na_2B_4O_7$ solutions

A.Diab[1,2]*, M.S.El-Attar[1,2], S.Abd El Wanees[1,3]

[1]Chemistry Department, Faculty of Science, Zagazig University, Zagazig, (EGYPT)

[2]Medical Chemistry Department, Faculty of Preparatory Year, Gizan University, Gizan, (KINGDOM OF SAUDI ARABIA)

[3]Chemistry Department, Faculty of Science, Tabuk University, Tabuk, (KINGDOM OF SAUDI ARABIA)

E-mail: ahmeddeiab@yahoo.com

ABSTRACT

The formation and growth of an oxide film on indium electrode immersed in sodium borate solutions has been followed and discussed using potential measurements under open-circuit conditions. The effect of concentration, pH and temperature of solution are also investigated. It is found that, the rate of oxide film growth follows a direct logarithm law, as evident from the linear relationship between the open-circuit potential and the logarithm of immersion time. The rate of oxide film growth decreases by increasing the pH of solution and by raising the solution temperature. The free activation energy of oxide film growth is determined and found to be 8.88 kJ/mole, indicating that the process of oxide film growth is under diffusion control.

KEYWORDS

Indium;
$Na_2B_4O_7$;
Oxide film thickening;
Polarization.

INTRODUCTION

Indium and its alloys are widely used in everyday practice; primarily as commercial applications in opto-electronics and alkaline batteries to suppress gassing and as an anti-arcing additive in high current electrical switches and contactors[1-5]. In, Pb–In and Bi–In have been investigated as potential materials as negative battery electrodes[6]. However, most of the attention has been focused on research related to indium oxide films, owing their great industrial importance, while, on the other side, the properties of pure indium metal have been rarely investigated. Indium oxide is a n-type semiconductor and as such is used as resistive element in integrated circuits and to form hetero junctions with p-InP, n-GaAS and other semiconductors. When In_2O_3 is doped with tin dioxide (SnO_2), thin films of indium-tin oxide (ITO) function as a transparent electrical conductor and have been widely used in a variety of opto-applications such as liquid crystal displays (LCDs), energy- efficient windows, solid-state image sensors, solar cells, and cathode ray tubes (CRTs)[6-8]. The major use of indium oxide is in the manufacture of ITO sputtering targets for thin film coating by compacting a mixture of indium oxide and tin dioxide powders. Most common methods of indium oxide and indium-tin oxide (ITO) film preparation are reactive deposition technique in a vacuum deposition unit[6, 9-13], thermal deposition[6, 14-15], and solution growth[6, 15–18]. The opto-electronic and structural properties of indium oxide films have also been widely investigated[4–16], while Okada et al. [17] investigated a possibility of using indium oxide as a mate-

rial for the oxygen electrode in electrochemical devices with a solid oxide electrolyte. Vaishnav et al.[18] and Cheng-Wei Lin et al.[19] investigated the use of indium oxide thin films in the gas sensor technology.

However, the electrochemical properties of indium in electrolyte solutions are rather poorly known. The electrochemical properties of indium and anodically formed indium oxide films in electrolyte solutions have not been widely investigated. One of the most interesting aspects of anodic oxide ûlms on indium is that they can be reversibly 'switched' between electronically insulating and metal conducting states by varying the applied potential. The anodic and cathodic behavior of these ûlms is consistent with their rectiûcation or *n*-type semiconductor properties[6, 20].

Different electrochemical techniques has been used by Omanovic and Metikos-Hukovic[21] to study the formation and growth of a thin oxide film on polycrystalline indium in a borate buffer solution. Complex structural characterizations of the anodically formed indium oxide film have been studied using galvanostatic[21], cyclic voltammetry and impedance spectroscopy[22] techniques. It has been found that the behavior of indium during anodic oxidation resembles in many aspects the kinetics of anodization of valve metals (e.g. Ta, Zr, Ti, Al, Sb, Bi). This conclusion has been deduced from the linearity between the current density and (i) the oxide formation rate ; (ii) the reciprocal capacity (the unitary formation rate); (iii) the potential drop across the oxide layer. The kinetics and chemical stability of potentiostatically formed indium oxide ûlms were discussed by Saidman et al.[23] as a function of potential domain, time diffusing process, and hydroxide concentration. It has been concluded that the surface indium oxide film undergoes reductive decomposition to pure metallic indium in the solid phase, via the solid-state mechanism[23]. Thus, it is possible to generate an oxide-free indium surface in situ, by applying a sufficiently negative potential. This, together with the fact that indium has a large hydrogen evolution overpotential, is the basis for a possible application of indium as a cathode catalyst material[24]. Saidman et al.[23, 25] also discussed the kinetics and chemical stability of potentiostatically formed oxide films as a function of potential domain, time diffusing process, and hydroxide concentration. Munoz and Bessone[26] reported on the cathodic behavior of indium in the presence of chloride ions. The hydrogen evolution reaction and the effects of local alkalization, Cl^- ions concentration and the presence of surface oxide were analyzed. The data show the presence of a cathodic current density plateau (cd), this latter being attributed to a possible catalytic effect exerted by the oxide layer on the hydrogen evolution reaction. An increase of Cl^- ions concentration generates a shift of the cd plateau towards lower cathodic cd values. The appearance of a rise in the anodic cd at a potential close to -1.1 V was found to be dependent of the Cl^- ions concentration and to be controlled by mass transfer.

The aim of the present work is to shed more light on the oxide film formation and growth on an indium electrode in sodium borate solutions. The effect of the some factors, e.g., solution concentration ($1 \times 10^{-4} - 1 \times 10^{-1}$ M), and pH (9.13-11.49), as well as, temperature changes (25-55°C) on the initial rate of oxide film growth are examined.

EXPERIMENTAL

Open-circuit potential measurements

The working electrode was made from 99.99% pure indium rod 0.35 cm thick (Aldrich). The electrode was fixed to borosilicate glass tubes with epoxy resin so that the total exposed surface area was 0.38 cm^2. Electrical contacts were achieved through thick copper wires soldered to the ends of the indium rod not exposed to the solution. Before being used, the indium electrode was abraded into uniform surfaces by a grinding machine (model Jean Wirtz TG 200, Germany) using successive 0-, 00- and 000- grades emery papers, rinsed with acetone and finally washed with triply distilled water before immersing in the test solution.

The potential of the indium electrode was measured for a period of 3 h to the nearest mV on a Wenking potentiometer type PPT 70 relative to the saturated calomel electrode (SCE). For each solution concentration, duplicate measurements of the electrode potential were carried out and the mean value of the two readings was taken in consideration. The scatter in electrode potential measurements was evaluated as less than ±10 mV. The steady-state potentials were considered as those values which did not change by more than 1

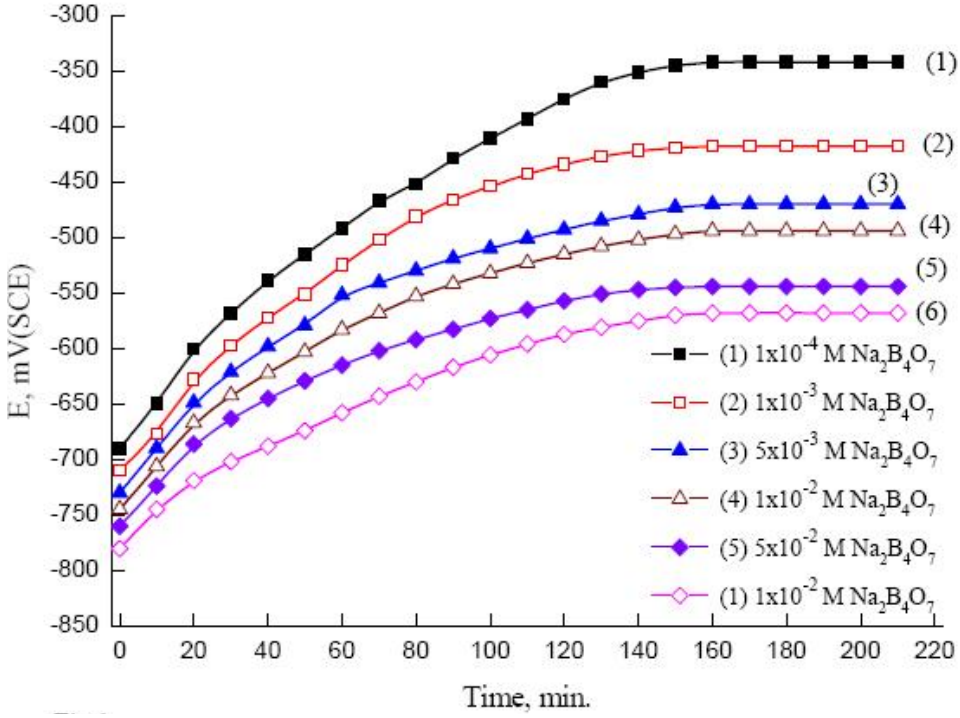

Figure 1 : Variation of the open-circuit potential, E, of the indium electrode with time, in naturally aerated $Na_2B_4O_7$ solutions of different concentrations.

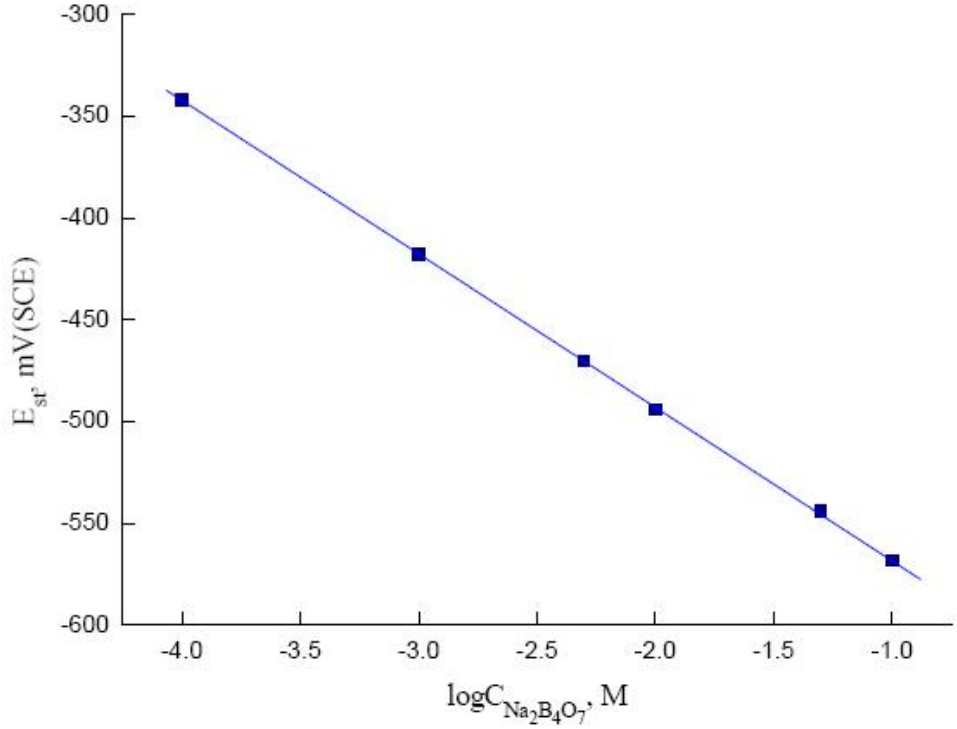

Figure 2 : Variation of the steady-final potential, E_{fin}., of the indium electrode with the logarithm concentrations of naturally aerated $Na_2B_4O_7$ solutions.

mV in 10 min. In some sets of experiments, the immersion time was extended to more than two days and the state steady potential was not changed by more than ± 20 mV.

Electrolytic solutions were prepared from analytical grade reagents and triply-distilled water. Solutions

Full Paper

of $Na_2B_4O_7$ with different concentrations were prepared by dissolving the corresponding quantitative weights of solid $Na_2B_4O_7$ in the appropriate volumes of distilled water. The pH of the solution was adjusted by dropwise addition of NaOH solution using an Orion Research Expandable Ion Analyzer EA 920. The cell has a double wall jacket through which water, at the adjusted temperature, was circulated. Measurements were carried out at a constant temperature 25± 0.1°C, except those related to the effect of temperature. The cell temperature was controlled using an ultra thermostat type polyscience (USA). The main joint of the cell contains openings for both the indium electrode and the reference electrode (SCE). No trails were made to measure the oxygen content of the solution.

RESULTS AND DISCUSSION

Effect of $Na_2B_4O_7$ concentration

The passivation behaviour of indium in $Na_2B_4O_7$ solutions of different concentrations is followed by measuring the open-circuit potential of In electrode as function of time until steady-state potentials are reached. The curves of Figure 1 represent such behaviour in $Na_2B_4O_7$ solutions of concentrations varying between $1x10^{-4}$ M and $1 x 10^{-1}$ M. Inspection of the curves of this figure reveals that, the steady-state potentials, E_{st}, in all solutions concentrations are invariably approached from more negative values following the immersion of the electrode in solution and attain constancy after a period of ~3 h. Also, in all solutions of different concentrations of $Na_2B_4O_7$, E_{st} tends towards more negative values as the concentration of $Na_2B_4O_7$ is increased. The steady state potential, E_{st}, varies with the logarithm of the molar concentration of $Na_2B_4O_7$, Figure 2, according to a straight line relation[27-29]:

$$E_{st} = a_1 - b_1 \log C_{Na2B4O7} \quad (1)$$

where a_1 and b_1 are constants which depend on the solution concentration and the metal under test. The value of the constant a_1 = - 642 mV (SCE) represents the steady state potential of In electrode, E_{st}, in 1 M $Na_2B_4O_7$ solution and b_1 amounts to 75 mV/min. The literature showed similar behavior for other metals, e.g., Zn[29], Ni[27], Zn alloy[30], Fe[31] and steel[28].

The ennobling of the In electrode potential when immersed in naturally aerated $Na_2B_4O_7$solutions denotes that the pre-immersion oxide film carried by the metal surface is not sufficient to impart passivity[27]. Healing and thickening of the film continue until passivity is reached. The open-circuit potential of the electrode reaches steady values after a time ranging from <"180 to 200 min. This finding can be explained on the basis of the continuous growth of the oxide film on the electrode surface[28]. Under these conditions, it is concluded that the cathodic reactions predominate over the anodic ones[27, 31]. In solutions exposed to a supply of oxygen, the most common cathodic reaction is the reduction of oxygen to hydroxyl ions. This can occur through either an increase in the self-polarization of the anodic areas or a decrease in the self- polarization of the cathodic ones. Here, the reduction of O_2 represents the most probable reaction accounting for the partial cathodic process of corrosion. Reduction of oxygen takes place in the overall reaction:

$$O_2 + 2H_2O + 4e' \rightarrow 4\ OH^- \quad (2)$$

The complementary anodic process whose released electrons sustain reaction (2) may be furnished from the ionization of In atoms entering the passive oxide phase, reaction (3), and/or is assumed to be released in accordance to Pourbaix[32] and Omanovic and Metikos-Hukovic[6], reactions (4 and 5), according the following reactions:

$$In \rightarrow In^{3+} + 3\ e^- \quad (3)$$

$$2\ In + 3\ H_2O \rightarrow In_2O_3 + 6\ H^+ + 6\ e^- \quad (4)$$

$$2\ In + 6\ OH^- \rightarrow In_2O_3 + 3\ H_2O + 6\ e^- \quad (5)$$

In^{3+} ions entering the oxide phase under the influence of an anodic current that polarizes the electrode and shifts its potential in the noble direction.

Omanovic and Metikos-Hukovic[22] found that the growth of the barrier oxy-hydrate layer occurs via a base catalyzed hydrolysis of the surface oxide film. Transformation from a gel-like oxide structure, InOOH, into the thermodynamically favorable and more stable crystalline form, In_2O_3, takes place at high positive potentials. In_2O_3 was found to expose high electric conductivity, which was manifested through oxygen evolution on its surface.

The way by which the oxide develops on the indium metal is best understood by presenting the results of potential –time on semi-logarithmic plots. As can be

seen from the curves of Figure 3, the open circuit potential of the In electrode was found to vary with the logarithm of the immersion time, *t*, in all $Na_2B_4O_7$ solution concentrations, according to[27-29, 31, 33-35]:

$$E = a_2 + b_2 \log t \quad (6)$$

where a_2 and b_2 are constants. The value of the constant b_2 which is the rate of potential rise (expressed as $\partial E/\partial \log t$) has actually decreased slightly with increasing the $Na_2B_4O_7$ concentration. Such behavior indicates that the oxide film thickening on the In electrode, under the prevailing experimental conditions, follows a direct logarithmic law.

The more interesting feature of the curves of Figure 3 is the fact that the *E*-log *t* curves are composed of two distinguished segments before reaching the final steady-state potentials. The first segment of these curves represents the first 50 minutes of immersion of the metal in the test solution; the rate of potential build-up is low. The slopes of these parts of the curves are dependent on the concentration. After definite, fairly-reproducible times, the rate of potential change (second segment) increases appreciably. The slope of both segments decreases with increasing the concentration indicating decreased rate of oxide film formation. The break in the *E*-log *t* relation may be related to the duplex nature of the formed oxide film on the indium surface[29]. Similar behavior is recoded before with zinc[29], titanium[36] and iron-chromium-nickel alloy[37]. Abd El Kader attributed this behavior to either formation of a more stable oxy-hydroxide film capable of existing in the aqueous solution, or to the formation of a new type of oxide film, probably porous modification, on the top of a compact barrier-type in contact with the metal surface[27].

However, it has been suggested before[29] that the driving force of the surface oxide film formation on metal is the free energy change of the reaction between metal and the test solution. This reaction is assumed to proceed by migration of metal cation and/or oxygen ion vacancies from metal towards the electrolyte or possibly by migration of negative oxygen ion in opposite direction[29, 38]. The field in oxide film is assumed to decrease as the oxide thickness on the metal increases until a steady film thickness is reached, where a steady-state potentials is attained. The relation governing the influence of electric filed, *H*, and ion transport is expected to follow the familiar Gunthereschulze and Betz relationship[39]:

$$i_a = k_a \exp(BH) \quad (7)$$

where i_a is the imposed anodic current density, k_a and *B* are constants, and *H* is the effective field strength. The idea was presented that under open circuit conditions, i_a can originate from the specific adsorption of anions on the oxide covered metal[37]. This would creates image charges of the same magnitude but of opposite sign at the oxide/metal interface, sufficient to promote ion transfer through the oxide to the film/solution interface.

It was further suggested that *H* in equation (7) could be replaced is by the quantity E/δ, where *E* is the measured potential relative to the suitable reference half cell, and δ is the thickness of the oxide film. The change of electrode potential to more positives values would necessitate a corresponding equivalent increase in the thickness of the oxide film, so as to keep the field strength E/δ, constant. Following this reasoning an equation was derived which describes the variation of the open-circuit potential of metal carrying very thin oxide film, *E*, with time, *t* [27] viz,

$$E = \text{const.} + 2.303\delta^-/B \log t \quad (8)$$

where δ^- represents the rate of oxide film thickening per unit decade of time, and *B* is a constant which is identified as[40]:

$$B = (nF/RT)\alpha\,\delta' \quad (9)$$

where α is the transfer coefficient similar to that encountered in normal electrochemical reactions[40], ($0 < \alpha < 1$) and δ' is the width of the energy barrier surmounted by the ion during transfer. From the values of the slopes of the straight lines of Figure 3, relating the variation of *E* with log *t*, one readily calculate the values of the rate of oxide thickening, δ^-, in $Na_2B_4O_7$ solutions of different concentrations. By analogy with the case of iron-chrome[37] and aluminium[41] we assume that trivalent cations diffuse through the film to oxide film interface. The constant n in equation (9) is set equal to 3, and *B* acquires the value 58.9 nmV^{-1}. The values of δ^- thus obtained are listed in TABLE 1.

In Figure 4, the values of the rate of oxide thickening, δ^-, (nm per unit decade of time) are plotted as function of the logarithm of $Na_2B_4O_7$ concentration. A straight line is obtained having a slope of 0.5 nm/ unit

Full Paper

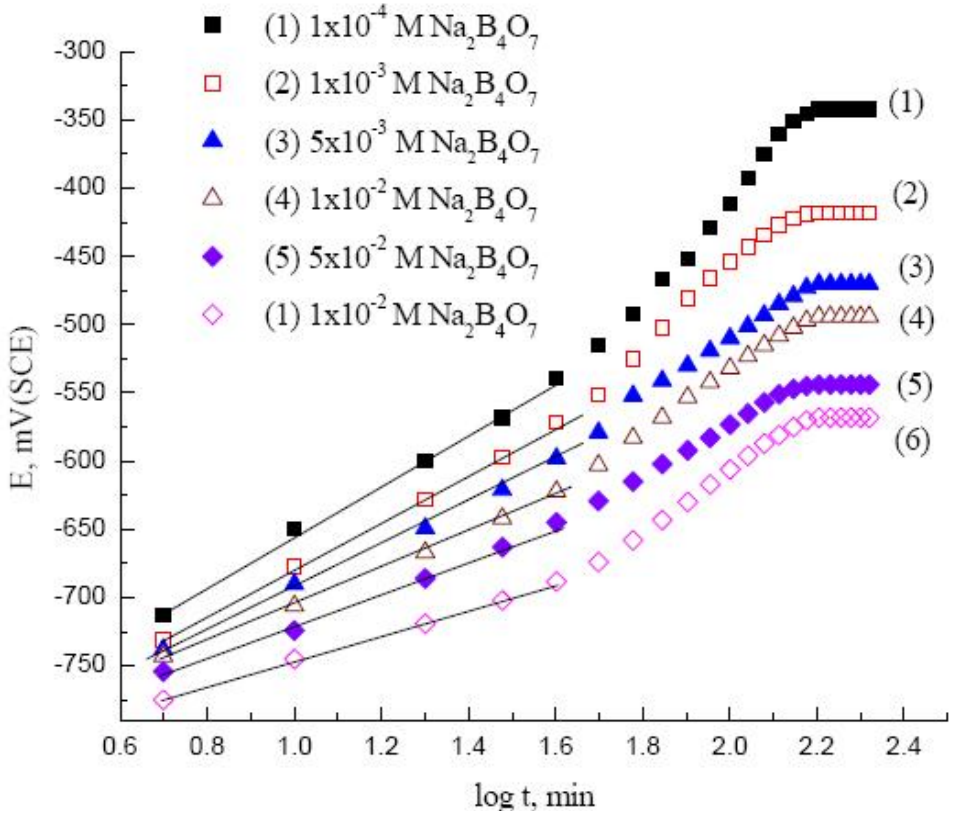

Figure 3 : Variation of the open-circuit potential, E, of the indium electrode, in naturally aerated $Na_2B_4O_7$ solutions of different concentrations, with the logarithm of immersion time, t.

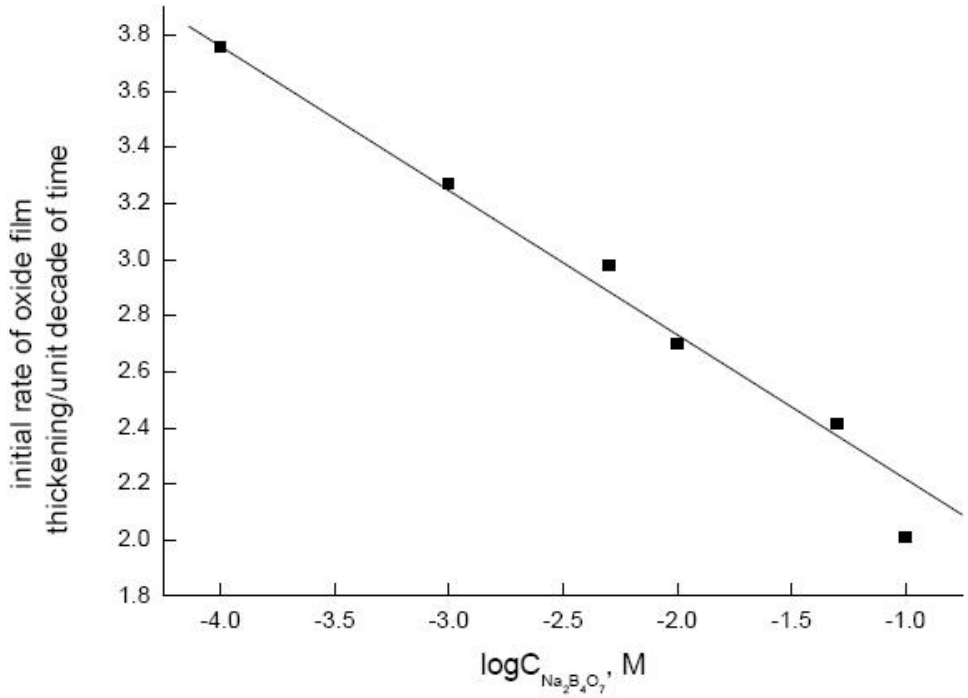

Figure 4 : Variation in the initial rate of oxide thickening, $\delta^{\cdot}$, with the concentration of naturally aerated $Na_2B_4O_7$ solutions.

decade of time.

Inspection of the curves of Figure 3 and 4 reveals that the initial rate of oxide film thickening of the indium electrode, under examination, in naturally aerated solu-

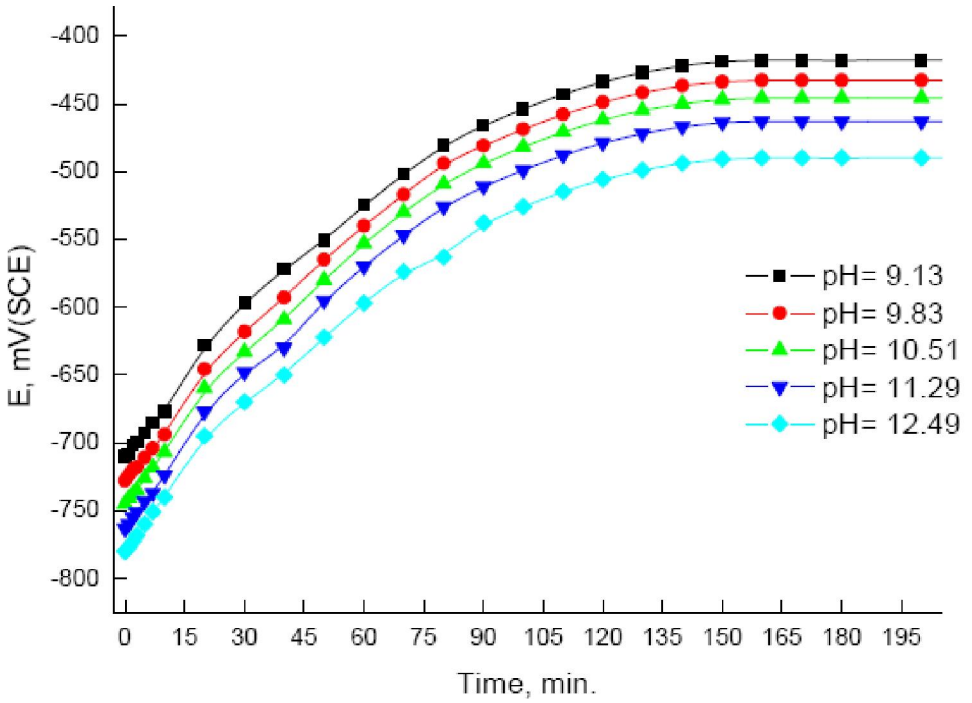

Figure 5 : Variation of the open-circuit potential, E, of the indium electrode with time, in naturally aerated 1x10^{-3}M $Na_2B_4O_7$ solutions at different pH values.

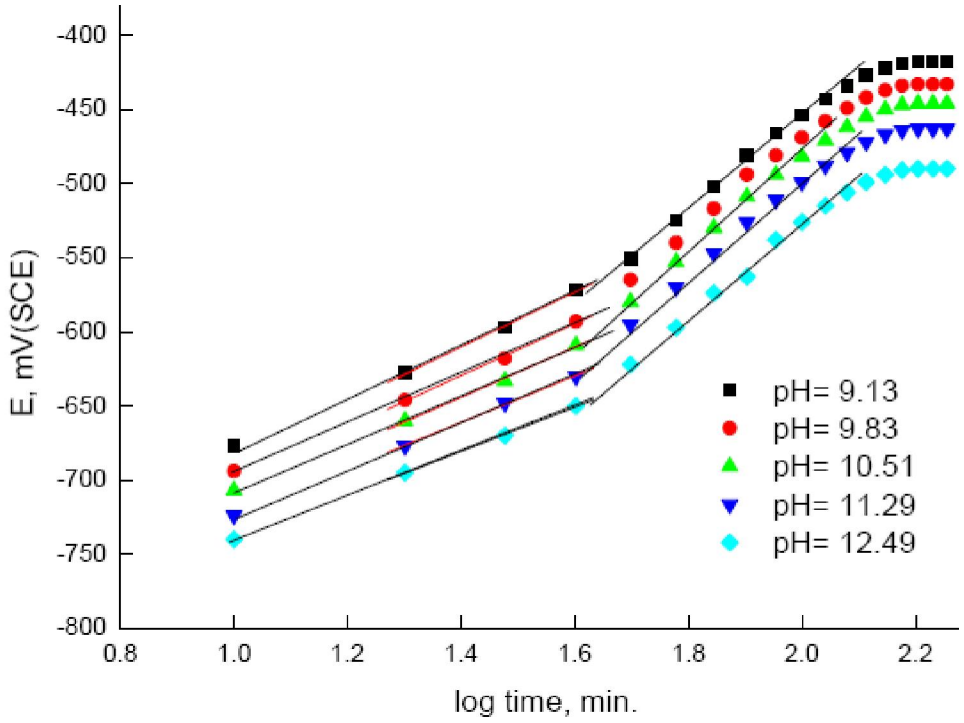

Figure 6 : Variation in the steady-final potential, E_{fin}., of the indium electrode, in naturally aerated 1x10^{-3}M $Na_2B_4O_7$ solutions, with the pH of the solution.

tions of $Na_2B_4O_7$ decreases with increasing the concentration of solution until reaching the steady state value. From the slopes of the straight line relationship of Figure 4, a tenfold increase in the concentration of $Na_2B_4O_7$ causes a decrease in the initial rate of oxide film thickening by only 0.5 of oxide film thickening.

When indium immersed in aqueous solution, an indium oxide film is formed due to the lower energy of

Full Paper

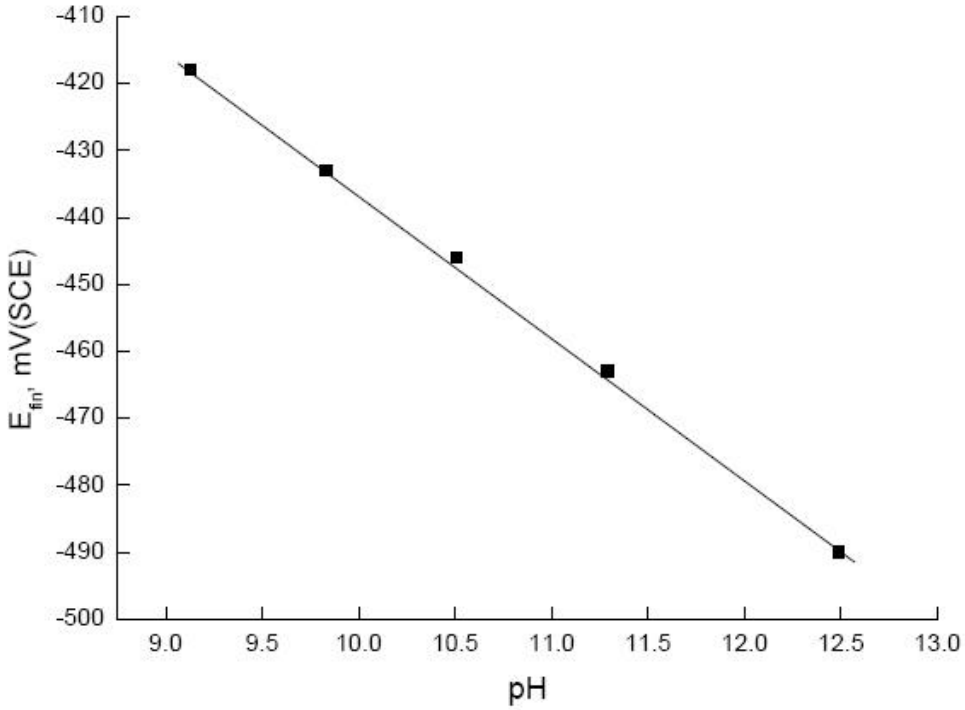

Figure 7 : Variation of the open-circuit potential, E, of the indium electrode, in naturally aerated 1x10^{-3}M $Na_2B_4O_7$ solutions at different pH values, with the logarithm of time, t

the In^{+3}-"O bond, which diffuse easily to reach the oxide/electrolyte interface[43]. In an alkaline borate solution the anodic behavior of indium lead to formation of a thin indium oxide film[22]. This process was found to be under a mixed control including an initial stage of an In-oxide formation involves a faster charging process and a slower surface diffusion process, with an effective diffusion coefficient of 10^{-15} cm^2 s^{-1}. On the top of this layer, which is of monolayer dimensions, the growth of the barrier oxy-hydrate layer occurs via a base catalyzed hydrolysis of the surface oxide. Transformation from a gel-like oxide structure (InOOH) into the thermodynamically favorable and more stable crystalline form (In_2O_3) takes place at high positive potentials. In_2O_3 was found to expose high electric conductivity, which was manifested through oxygen evolution on its surface[42].

Effect of pH

The curves of Figure 5 represent the variation of the open-circuit potential of indium electrode with time in naturally aerated 1x10^{-3} M $Na_2B_4O_7$ solutions of different *pH* values, at 25°C. These solutions has *pH* varies between 9.13 and 11.49, which are adjusted by the dropwise addition of NaOH solution. The curves have the general features, similar to those of Figure 1A. As was previously noted, the steady potentials are reached from negative values indicating the ennobling of the indium potential with time, which decreases with raising the *pH* of solution. The steady potential, E_{st}, varies with the *pH* of solution, Figure 6, according to the relation:

$$E_{st} = a_3 - b_3\, pH \qquad (10)$$

where a_3 and b_3 are constants; the constant b_3 having a value -21.34 mV/pH unit. The shift of the steady state potential, E_{st}, of the indium electrode in the negative direction with increasing the *pH* of solution, Figure 5 and 6, could be attributed to the partial dissolution of the passive oxide film with increasing the alkalinity of the medium according to.

$$In(OH)_3 + OH^- = In(OH)_4^- \qquad (11)$$

The curves in Figure 7 represent the variation of the open-circuit potential of the indium electrode, in solution of different pH's, as function of the logarithm of the immersion time, *t*. invariably straight lines are obtained at different *pH* values. As can be seen from these curves, the slope of the straight lines obtained is very slightly decreased with raising the pH of solution. In Figure 8, however, the change of the initial rate of oxide film thickening, as calculated from Eqs. (3) and (4), with the pH of solution is depicted. From the value of

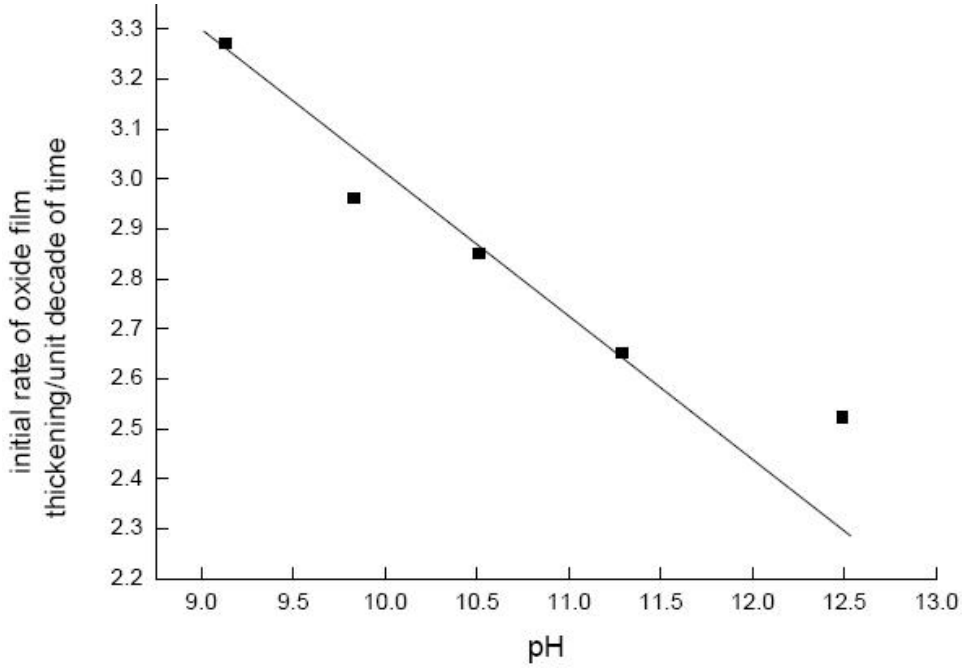

Figure 8 : Variation in the initial rate of oxide thickening, δ^-, of the indium electrode in, naturally aerated 1x10^{-3}M $Na_2B_4O_7$ solutions, with the pH of the solution.

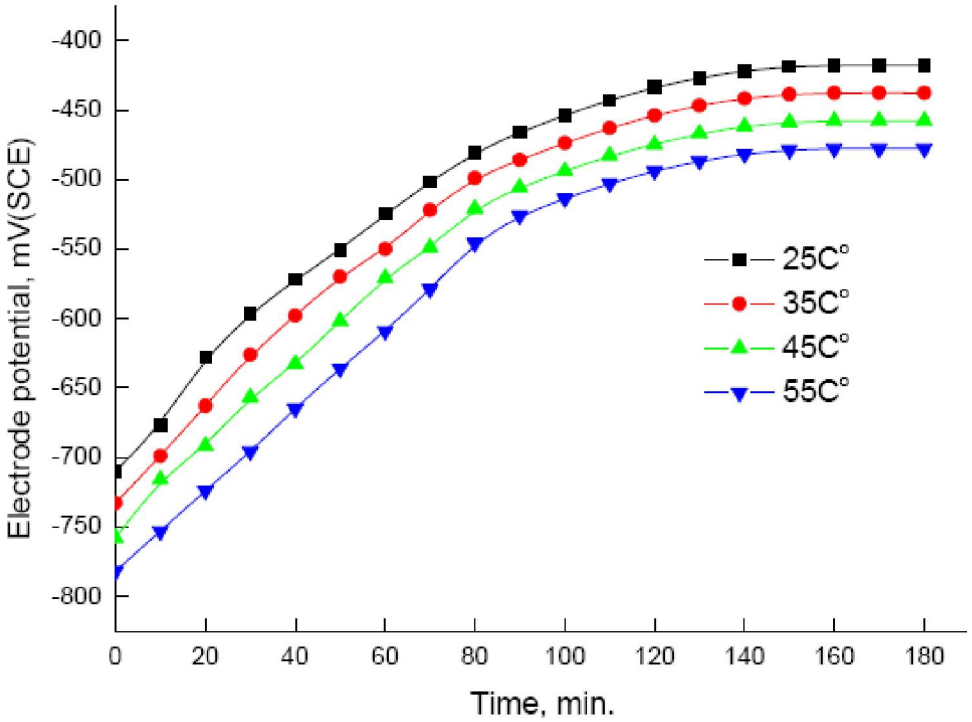

Figure 9 : Variation of the open-circuit potential, E, of the indium electrode with time, in naturally aerated 1x10^{-3}M $Na_2B_4O_7$ solutions, at different temperatures.

the slope of the straight line of Figure 8, this amounts to be ~ 0.26 nm/unit decade of time/ pH decade. It is quite clear that, the increasing of the pH value of naturally aerated 1x10^{-3} M $Na_2B_4O_7$ solution by one unit decreases the initial rate of oxide film thickening on the indium surface by only 0.26 nm/unit decade.

Metikos-Hukovic et al.[22] stated that, at high region of pH, the oxide growth occurs presumably via a base catalyzed hydrolysis, by incorporation of water molecules (i.e. OH species) through the pores into the

Full Paper

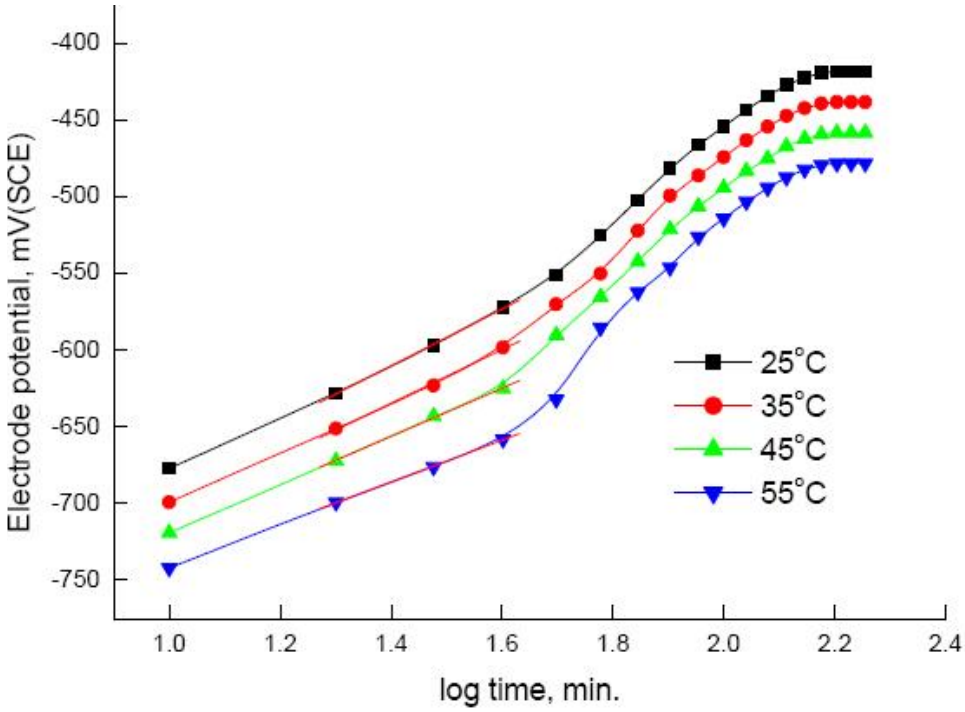

Figure 10 : Variation in the steady-final potential, E_{fin}., of the indium electrode in naturally aerated $1x10^{-3}$M $Na_2B_4O_7$ solutions, with the temperature.

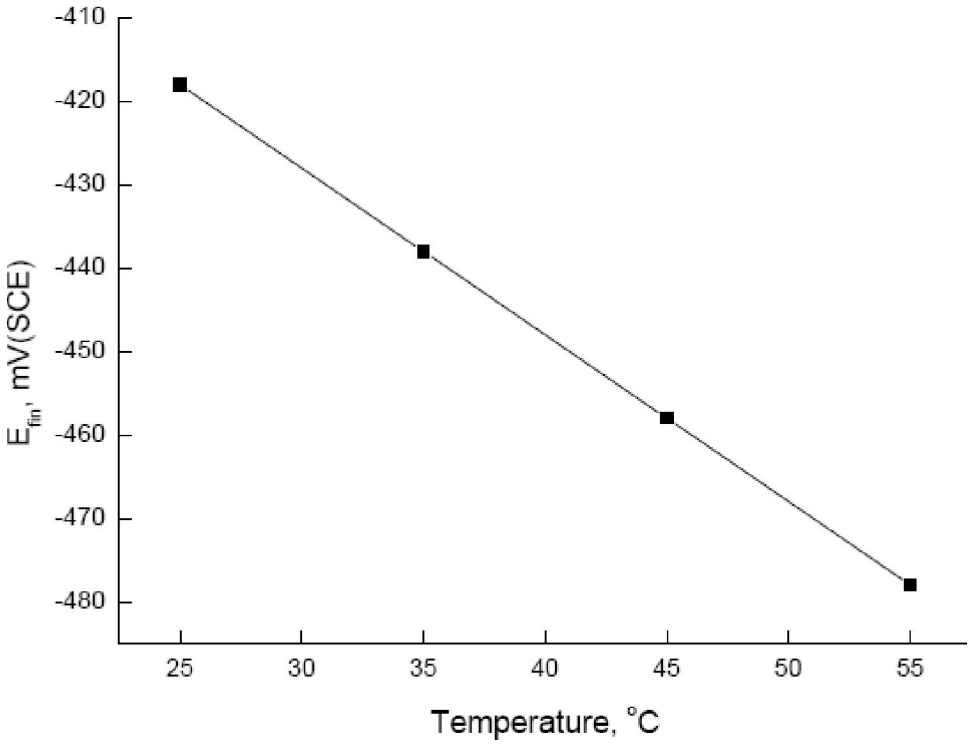

Figure 11 : Variation of the open-circuit potential, E, of the indium electrode, in naturally aerated $1x10^{-3}$M $Na_2B_4O_7$ solutions at different temperatures with logarithm the time, t.

film. It is assumed that this surface deterioration proceeds preferentially at grain boundaries and dislocations, taking advantage of the instability of the crystal lattice at these points. The final result is formation of a highly hydrated InOOH oxide film. Thus, the oxide film composition and structure strongly depend upon the

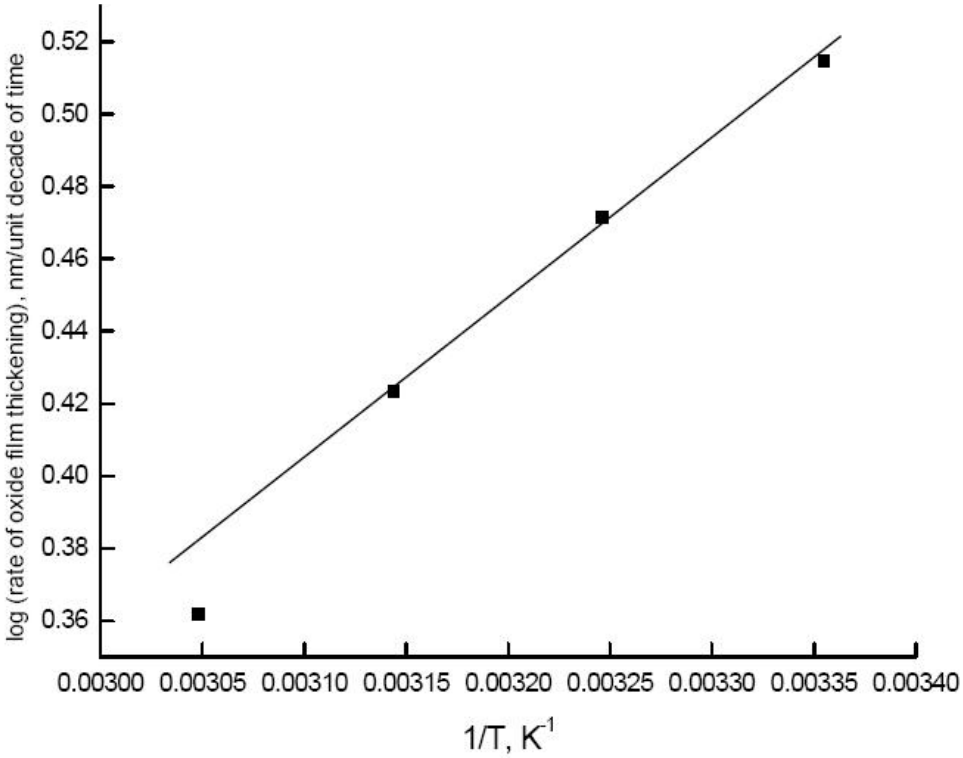

Figure 12 : Variation in the initial rate of oxide thickening, δ^-, of the indium electrode, in naturally aerated $1x10^{-3}$M $Na_2B_4O_7$ solutions with 1/T, K^{-1}.

OH^- ion concentration available at the reaction sites. The same behavior was noticed during the potentiodynamic passivation of tin, antimony and zinc[44-47].

El Sayed et al[48] suggested that, with increase the alkalinity of the medium there was a competition between anodic film formation and its chemical dissolution. It is probable that the anodic dissolution of indium in alkaline solution depends upon the diffusion of OH^- ions through the anodic oxide layer.

Effect of temperature

The curves of Figure 9 represent the variation of the open-circuit potential of the indium electrode, E, with time in naturally aerated $1x10^{-3}$ M $Na_2B_4O_7$ at temperatures varying between 25 and 55 °C. Inspection of the curves of this figure reveals that raising the solution temperature is accompanied by a marked effect on the value of the steady state potential, E_{st}. The latter varies with temperature in according with the straight line of Figure 10. It is quite clear that raising the temperature decreases the initial rate of oxide film growth or enhances the corrosion of the indium and the extent of corrosion promotion increases with raising the temperature, as reflected by the shifting of the final steady potential in the negative direction by 2 mV/ degree. This could be attributed to the decrease of solution viscosity and the consequent increase in the mobility of ions with raising the solution temperature[46]. The straight lines present in Figure 11 relate the variation of the open-circuit potential of the indium-electrode with the logarithm of the immersion time, t, in aerated $1x10^{-3}$ M $Na_2B_4O_7$ solutions, at temperatures ranging from 25 to 55 °C. The slopes of these straight lines decrease with raising the temperature. The calculated values of the initial rate of oxide film thickening on the indium electrode, at varying temperatures, are plotted as function of 1/T (K) in Figure 12. From the Arrhenius plots of this figure; the free activation energy of oxide film thickening on indium surface is computed to be 8.88 kJ/ mole. This low value of activation energy (< 40 kJ/mole) indicates that the process of oxide film thickening on the indium electrode is under diffusion control[47, 49, 50].

CONCLUSIONS

From the measurements of the open-circuit poten-

tial measurements of the indium electrode in naturally aerated $Na_2B_4O_7$ solutions, the following conclusions could be drawn:

(1) The steady potentials, E_{st}, are approached from negative values indicating oxide film healing and thickening.

(2) E_{st} varies with $Na_2B_4O_7$ concentration according to:

$E_{st} = a_1 - b_1 \log C_{Na2B4O7}$, where a_1 and b_1 are constants, accounting for the partial dissolution of the oxide film.

(3) The initial rate of oxide film thickening follows a direct logarithm law, as evident from the variation of the open-circuit potential, E, with log t; where $E = a_2 + b_2 \log t$.

(4) The initial rate of oxide film thickening decreases with increasing the concentration and pH of solutions and by raising the temperature due to the partial dissolution of the oxide film.

(5) The free activation energy of oxide film thickening is calculated and found to be 8.88 kJ/mole, indicating that the process of oxide film growth is under diffusion control.

REFERENCES

[1] T.Minami; "Present status of transparent conducting oxide thin-film development for Indium-Tin-Oxide (ITO) substitutes", Thin Solid Films, **516**, 17, 5822-5828 **(2008)**.

[2] J.Van Der Tol, R.Zhang, J.Pello, F.Bordas, G.Roelkens, H.Ambrosius, P.Thijs, F.Karouta, M.Smit; "Photonic integration in indium-phosphide membranes on silicon", IET Optoelectron., **5**, 218–225 **(2011)**.

[3] S.Ilican, Y.Caglar, M.Caglar, B.Demirci; " Polycrystalline indium-doped ZnO thin films: preparation and characterization", Journal of Optoelectronic and Advanced Materials, **10**, 2592–2598 **(2008)**.

[4] V.Ganesh, S.Farzana, S.Berchmans; "Nickel hydroxide deposited indium tin oxide electrodes as electrocatalysts for direct oxidation of carbohydrates in alkaline medium", J.Power Sources, **196**, 9890-9899 **(2011)**.

[5] S.S.Shinde, P.S.Shinde, C.H.Bhosale, K.Y.Rajpure; "Optoelectronic properties of sprayed transparent and conducting indium doped zinc oxide thin films", J.Phys.D, Appl.Phys, **41**, 105-109 **(2008)**.

[6] S.Omanovic, M.Metikos-Hukovic; "A study of the kinetics and mechanisms of electrocrystallization of indium oxide on an in situ prepared metallic indium electrode", Thin Solid Films, **458**, 52-62 **(2004)**.

[7] S.S.Shinde, P.S.Shinde, C.H.Bhosale, K.Y.Rajpure; "Optoelectronic properties of sprayed transparent and conducting indium doped zinc oxide thin films", J.Phys.D, Appl.Phys., **41**, 105-109 **(2008)**.

[8] D.Dubreuil, J.Pierre Ganne, G.Berginc, F.Terracher; "Optical and electrical properties between 0.4 and 12 ìm for Sn-doped In_2O_3 films by pulsed laser deposition and cathode sputtering", Applied Optics, **46**, 5709-5718 **(2007)**.

[9] W.Qin, R.Philip Howson, M.Akizuki, J.Matsuo, G.Takaoka, I.Yamada; "Indium oxide film formation by O_2 cluster ion-assisted deposition", Materials Chemistry and Physics, **54**, 258-261 **(1998)**.

[10] B.Alterkop, N.Parkansky, R.L.Boxman, S.Goldsmith; "Influence of a parallel electric field on the conductivity of a growing indium oxide film", Thin Solid Films, **290(291)**, 10-12 **(1996)**.

[11] K.Ozasa, T.Ye, Y.Aoyagi; "Deposition of thin indium oxide film and its application to selective epitaxy for *in situ* processing", Thin Solid Films, **246**, 58-64 **(1994)**.

[12] M.Balestrieri, D.Pysch, J.-P.Becker, M.Hermle, W.Warta, S.W.Glunz; "Characterization and optimization of indium tin oxide films for heterojunction solar cells", Solar Energy Materials and Solar Cells, **95**, 2390-2399 **(2011)**.

[13] M.Balestrieri, D.Pysch, J.P.Becker, M.Hermle, W.Warta, S.W.Glunz; "Characterization and optimization of indium tin oxide films for heterojunction solar cells", Solar Energy Materials and Solar Cells, **95**, 2390-2399 **(2011)**.

[14] P.Thilakan, J.Kumar; "Reactive thermal deposition of indium oxide and tin-doped indium oxide thin films on inp substrates", Thin Solid Films, **292**, 50-54 **(1997)**.

[15] M.L.Mottern, F.Tyholdt, A..Ulyashin, A.T.J.Van Helvoort, H.Verweij, R.Bredese; "Textured indium tin oxide thin films by chemical solution deposition and rapid thermal processing", Thin Solid Films, **515**, 3918-3926 **(2007)**.

[16] S.J.Duncan, G.T.Burstein; "Kinetics of anodic oxide film growth on indium in alkaline solution", J.Appl.Electrochem., **17**, 196 -204 **(1987)**.

[17] K.Okada, S.Kohiki, S.Luo, D.Sekiba, S.Ishii, M.Mitome, A.Kohno, T.Tajiri, F.Shoji; " Correla-

tion between resistivity and oxygen vacancy of hydrogen-doped indium tin oxide thin films", Thin Solid Films, **519**, 3557-3561 **(2011)**.

[18] V.S.Vaishnav, P.D.Patel, N.G.Pate; "Preparation and characterization of indium tin oxide thin films for their application as gas sensors", Thin Solid Films, **487**, 277-282 **(2005)**.

[19] C.W.Lin, H.Ing Chen, T.Y.Chen C.-C.Huang, C-S- Hsu, R.-C.Liu, W.Chau; "On an indium–tin-oxide thin film based mmonia gas sensor", Sensors and Actuators B, Chemical, In Press, **(2011)**.

[20] H.S.Mohran, A.Rahman El Sayed, H.M.Abd El-Lateef; "Anodic behavior of tin, indium, and tin–indium alloys in oxalic acid solution", J.Solid State Electrochem, **13**, 1279–1290 **(2009)**.

[21] S.Omanovic, M.Metikos-Hukovic; "Oxide film growth on Al–In alloys in a borate buffer solution in conditions of galvanostatic anodising", Solid State Ionics, **78**, 69 **(1995)**.

[22] M.Metikos-Hukovic, S.Omanovic; "Thin indium oxide film formation and growth, Impedance spectroscopy and cyclic voltammetry investigations", J.Electroanal.Chem., **455**, 181-189 **(1998)**.

[23] S.B.Saidman, E.C.Bellocq, J.B.Bessone; "Stationary and non-stationary electrochemical response of polycrystalline indium in alkaline media," , Electrochim.Acta., **35**, 329-338 **(1990)**.

[24] S.Omanovic, M.Metikos-Hukovic; "Indium as a cathodic material, catalytic reduction of formaldehyde", J.Appl.Electrochem., **27**, 35-41 **(1997)**.

[25] S.B.Saidman, J.B.Bessone; "Anodic behaviour of indium in sodium chloride solutions", Electrochim.Acta., **36**, 2063-2067 **(1991)**.

[26] A.G.Munoz, J.B.Bessone; " Cathodic behavior of In in aqueous sodium chloride solutions", Electrochim.Acta., **43**, 2033-2040 **(1998)**.

[27] J.M.Abd El Kader, A.M.Shams El Din; "Film thickening on nickel in aqueous solutions in relation to anions type and concentration", Br.Corros.J., **14,** 40–45 **(1979)**.

[28] S.M.Abd El Haleem, E.E.Abd El Aal, S.Abd El Wanees, A.Diab; "Environmental factors affecting the corrosion behaviour of reinforcing steel, I.The early stage of passive film formation in $Ca(OH)_2$ solutions", Corros.Sci., **52**, 3875–3882 **(2010)**.

[29] E.E.Abd El Aal; Oxide ûlm formation on zinc in borate solutions in open circuit", Corrosion Science, **50**, 41–46 **(2008)**.

[30] M.Abd El Haleem, S.S.Abd El-Rehim; Corrosion behaviour of commercial Zn–Ti alloy in aqueous salt solutions", Revue-Rommanie Di Chimie, **25**, 493–501**(1980)**.

[31] E.E.Abd El Aal, S.M.Abd El Haleem; "Kinetics of oxide ûlm growth and destruction on iron surface in carbonate solutions", Corros.Engin.Science.and Techn., **43**, 219–224 **(2008)**.

[32] M.Pourbaix; Atlas of electrochemical equilibria in aqueous solutions, Pergamon press, Oxford, 436, **(1966)**.

[33] G.T.Burstein, R.M.Organ; "Repassivation and pitting of freshly generated aluminum surfaces in acidic nitrate solution", Corrosion Science, **47**, 2932–2955 **(2005)**.

[34] H.A.El Shayeb, F.M.Abd El Wahab, E.A.El Meguid; "Electrochemical behavior of molybdenum electrodes in various aqueous and buffered solutions and their use in titration, Br.Corros.J., **36**, 215–220 **(2001)**.

[35] G.T.Burstein, R.J.Cinderey; "Evolution of the corrosion potential of repassivating aluminium surfaces, Corrosion Science, **33**, 475–492 **(1992)**.

[36] J.M.Abd El Kader, F.M.Abd El Wahab, H.A.El Shayeb, M.G.A.Kader; Br.Corros.J., **16,** 111 **(1981)**.

[37] J.M.Abd El Kader, F.M.Abd El Wahab M.G.A.Kader, A.M.Shams El Din; "Oxide film thickening on the surface of iron chrome alloys in relation to anion type and concentration", Materials Chemistry, **7,** 313-330 **(1982)**.

[38] L.Young; Anodic oxide films, Academic Press, London, New York, 186 **(1961)**.

[39] A.Guntherschulze, H.Betz, Die Bewegung der ionengitter von isolatoren beiextremen elektrischen Feldstarken, Zeitschrift für Physik, **92**, 367–374 **(1934)**.

[40] K.J.Vetter, in, H.Fisher, K.Hanfe, W.Wederholt (Eds.); Pssivierende Filme und Deckschichten, Springer Verlag, Berlin, **72**, **(1956)**.

[41] S.M.Abd El Haleem, E.E.Abd El Aal, S.Abd El Wanees, A.Farouk; "Environmental factors affecting the corrosion behaviour of aluminium, I.

[42] S.Gudiæ**,** J.Radoševiæ**,** A.Višekruna, M.Kliškiæ; "Oxide film growth on Al–In alloys in a borate buffer solution in conditions of galvanostatic anodizing", Electrochim.Acta., **49**, 773-783 **(2004)**.

[43] L.C.A.Thompson, R.Pace; Journal of Inorganic and Nuclear Chemistry, **25**, 1041-104 **(1963)**.

[44] B.Bressel, H.Gerischer; Ber.Bunsenges.Phys.Chem., **87**, 398 **(1983)**.

[45] M.Spitler, M.Luebke, H.Gerischer,

Ber.Bunsenges.Phys.Chem., **83**, 663 **(1979)**.

[46] D.Pavlov, M.Bojinov, T.Laitinena, G.Sundholml; Electrochim.Acta., **36**, 2081 **(1991)**.

[47] M.Metikos'-Hukovic, R.Babic, S.Omanovic, J.Electroanal.Chem., **374**, 199 **(1994)**.

[48] A.El Sayed, S.S.Abd El Rehim, H.Mansour, Monatshefte für Chemie, **122**, 1019-1027 **(1991)**.

[49] S.S.Zumdahl; Chemistry, 3rd Edition., D.C.Heath & Co.,645 **(1993)**.

[50] A.Wieckowski, E.Ghali; On the interpretation of cyclic voltammograms of iron electrode in alkaline solution at elevated temperatures, Electrochimica Acta, **30**, 1423–1431 **(1985)**.